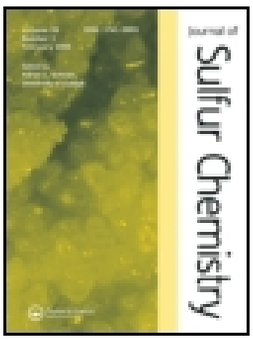

Journal of Sulfur Chemistry

ISSN: 1741-5993 (Print) 1741-6000 (Online) Journal homepage: http://www.tandfonline.com/loi/gsrp20

Silica-modified magnetite Fe_3O_4 nanoparticles grafted with sulfamic acid functional groups: an efficient heterogeneous catalyst for the synthesis of 3,4-dihydropyrimidin-2(1H)-one and tetrahydrobenzo[b]pyran derivatives

Davood Azarifar, Omolbanin Badalkhani & Younes Abbasi

To cite this article: Davood Azarifar, Omolbanin Badalkhani & Younes Abbasi (2016): Silica-modified magnetite Fe_3O_4 nanoparticles grafted with sulfamic acid functional groups: an efficient heterogeneous catalyst for the synthesis of 3,4-dihydropyrimidin-2(1H)-one and tetrahydrobenzo[b]pyran derivatives, Journal of Sulfur Chemistry, DOI: 10.1080/17415993.2016.1177055

To link to this article: http://dx.doi.org/10.1080/17415993.2016.1177055

JOURNAL OF SULFUR CHEMISTRY, 2016
http://dx.doi.org/10.1080/17415993.2016.1177055

Taylor & Francis
Taylor & Francis Group

Silica-modified magnetite Fe_3O_4 nanoparticles grafted with sulfamic acid functional groups: an efficient heterogeneous catalyst for the synthesis of 3,4-dihydropyrimidin-2(1*H*)-one and tetrahydrobenzo[b]pyran derivatives

Davood Azarifar, Omolbanin Badalkhani and Younes Abbasi

Faculty of Chemistry, Bu-Ali Sina University, Hamedan, Iran

ABSTRACT

Silica-modified magnetite-polyoxometalates functionalized with sulfamic acid groups as hybrid nanoparticles were prepared by sulfonation of diamine-functionalized propyl group grafted on the magnetic silica-coated Fe_3O_4 nanoparticles. This heterogeneous nanocatalyst was explored to present high catalytic performance for the synthesis of 3,4-dihydropyrimidinones and tetrahydrobenzo[b]pyrans under mild reaction conditions. The properties of this nanocatalyst were characterized by FT- infrared, energy-dispersive X-ray spectrum, scanning electron microscope, X-ray diffraction, X-ray fluorescence and elemental analysis. Easy separation of the nanocatalyst by using an external magnet, recyclability, non-toxicity, versatility and high stability of the catalyst combined with low reaction times and excellent yields make the present protocol very useful and attractive for the synthesis of the titled products.

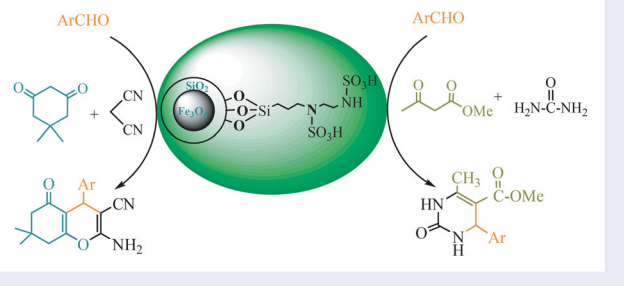

ARTICLE HISTORY
Received 29 November 2015
Accepted 27 March 2016

KEYWORDS
Heterogeneous nanocatalyst; magnetic nanoparticles; sulfonation; 3; 4-dihydro pyrimidin-2(1*H*)-one; tetrahydrobenzo[b]pyran

1. Introduction

In the past decade, many reports on the synthesis and applications of magnetic nanoparticles (MNPs) on different industrial and biological fields such as magnetic resonance

CONTACT Davood Azarifar azarifar@basu.ac.ir Faculty of Chemistry, Bu-Ali Sina University, Zip Code 65178, Hamedan, Iran

Supplemental data for this article can be accessed here. http://dx.doi.org/10.1080/17415993.2016.1177055

imaging, drug delivery, bioseparation, hyperthermia and catalytic processes have been published. Also, magnetic NPs have attracted much research interests as excellent supports for various catalysts which can be easily separated from the products simply by using an external magnetic field and recycled.[1–4] Moreover, the surface of magnetic metal oxide NPs such as magnetic Fe_3O_4 nanoparticles could be functionalized and modified by various organic and inorganic materials such as silica, polymers, biomolecules, metals, etc. which have been used as selective and efficient catalysts in a wide range of catalytic reactions.[5,6] Among these nanocatalytic systems, nano-oxide-supported functionalized polyoxometalates have emerged as useful catalysts in organic reactions.[7] These heterogeneous catalysts contain reactive sites with high mobility similar to those in homogeneous catalysts and can be easily recycled. Based on these preferences, different types of acids such as phosphotungstic acid ($H_3PW_{12}O_{40}$) and sulfonic acid have been grafted on the functionalized silica-coated Fe_3O_4 MNPs and are successfully used for selectively catalyzing chemical transformations.[7–11]

Among the important heterocyclic compounds, 3,4-dihydropyrimidin-2(1*H*)-ones and their derivatives are well-documented compounds which have attracted enormous synthetic interest due to their therapeutic, pharmacological and biological properties.[12] Many of these compounds exhibit vital medicinal properties such as antiviral, antibacterial, antitumor, antihypertensive, neuropeptide Y (NPY) antagonism and anti-inflammatory activities.[13] Amongst the most important drugs used, monastrol is a well-known medicine which acts as a specific inhibitor of mitotic kinesin Eg5 and is considered as a lead compound for the development of new anticancer drugs.[14] The most used methods for the synthesis of 3,4-dihydropyrimidin-2(1*H*)-ones are based on the three-component Biginelli condensation reaction between an aldehyde, urea or thiourea, and an easily enolizable carbonyl compound.[15,16] So far, many efficient and versatile catalytic approaches in the synthesis of 3,4-dihydropyrimidin-2(1*H*)-ones have been developed and scope for further developments toward milder reaction conditions and better selection of the catalyst and reaction components still exists.[17]

Another well-documented class of heterocyclic compounds of important pharmacological and therapeutic properties belongs to 4*H*-chromene derivatives which have received great attention in synthetic organic chemistry. Similarly, a large number of chromene derivatives perform different biological and pharmacological activities as spasmolytic, diuretic, anticoagulant, anticancer and anti-anaphylactic agents.[18] With respect to the importance of 4*H*-chromenes, different methods have been developed for the synthesis of these compounds employing various catalysts such as ionic liquids,[19] hexadecyl trimethyl ammonium bromide,[20] Mg/La-mixed metal oxides,[21] and nanosilica.[22] In addition, several other methods have been developed based on different conditions using reactants in solid or molten states,[23] and electrolysis condition.[24]

Following our previous reports on the synthesis of different heterocyclic compounds including 4*H*-chromenes and 3,4-dihydropyrimidinones using various catalysts such as nano-magnetic mixed lanthanum strontium magnesium oxide nanoparticles,[25] nano-titania-supported Preyssler-type heteropoly acid,[26] and under ultrasonic irradiation condition,[27] herein, we wish to report the one-pot three-component synthesis of the titled products employing sulfamic acid-functionalized magnetic Fe_3O_4 nanoparticles as an efficient and magnetically recoverable heterogeneous catalyst (Scheme 1).

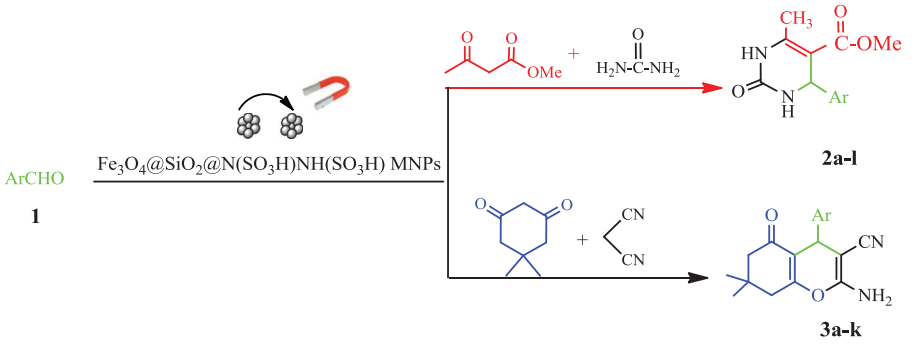

Scheme 1. Synthesis of 3,4-dihydropyrimidin-2(1*H*)-ones **2a–2l** and 4*H*-chromenes **3a–3k** catalyzed by Fe_3O_4@SiO_2@N(SO_3H)NH(SO_3H) MNPs.

2. Results and discussion

Our concept of supported amino sulfuric acid catalysis involves the surface of a nano-magnetic support material which is modified with a monolayer of covalently bonded organo amine sulfonic acid moieties. For our purpose, we have chosen, for the first time, to immobilize the sulfanilic acid groups on silica-modified magnetic Fe_3O_4 nanoparticles, Fe_3O_4@SiO_2@N(SO_3H)-NH(SO_3H). Following the previously reported method,[28] as illustrated in Scheme 2, in the first step, $FeCl_3{\cdot}6H_2O$ and $FeCl_2{\cdot}4H_2O$ were reacted in basic solution under ultrasonication to co-precipitate the Fe^{+2} and Fe^{+3} ions that resulted in the formation of Fe_3O_4 MNPs. In the second step, in order to protect the Fe_3O_4 NPs from possible oxidation or aggregation, a layer of SiO_2 was coated on the external surface of the Fe_3O_4 NPs by using the previously reported method.[29] Subsequently,

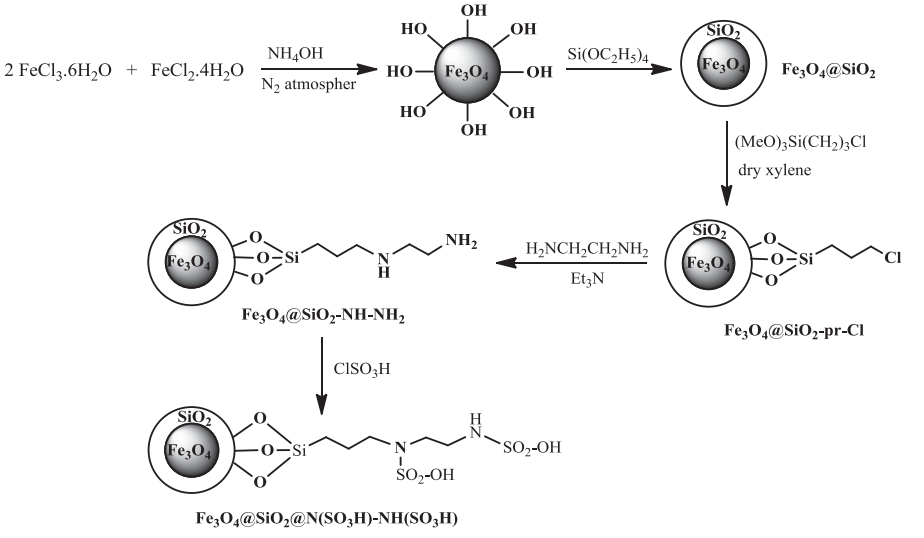

Scheme 2. Steps of the synthesis of the catalyst Fe_3O_4@SiO_2@N(SO_3H)-NH(SO_3H) NPs.

the silanol groups on the surface of Fe_3O_4@SiO_2 nanoparticles were treated with 3-chloropropyltrimethoxysilane to obtain Fe_3O_4@SiO_2-Cl. Then, the resulted chloropropyl-grafted Fe_3O_4@SiO_2 was reacted with ethylenediamine to obtain Fe_3O_4@SiO_2@NH-NH_2 MNPs. In the final step, the sulfonation of the both amine groups in Fe_3O_4@SiO_2@NH-NH_2 was implemented by reaction with chlorosulfonic acid under ultrasonication to yield the N,N′-disulfonated MNPs Fe_3O_4@SiO_2@N(SO_3H)-NH(SO_3H).

The characterization of the catalyst was performed by elemental, Fourier transform infrared (FT-IR), energy-dispersive X-ray spectrum (EDX), scanning electron microscope (SEM), X-ray diffraction (XRD) and X-ray fluorescence (XRF) analyses. The elemental analysis showed that the carbon, hydrogen, nitrogen and sulfur contents of the prepared catalyst were 6.04, 1.04, 2.40 and 9.36 (wt%), respectively. This analysis confirms a loading of 2.92 mmol of sulfonic acid groups per gram of the support, and indicative of the successful sulfonization of the both amino groups in the prepared Fe_3O_4@SiO_2-NH-NH_2 NPs.

The FT–IR spectra of the Fe_3O_4 NPs, chloropropyl-grafted Fe_3O_4@SiO_2 and the catalyst Fe_3O_4@SiO_2@N(SO_3H)-NH(SO_3H) are shown in Figure 1. In these spectra, the peaks exhibited, respectively, at 570, 583 and 597 cm^{-1} are ascribed to Fe–O stretching vibration. In addition, the sharp bands appearing at 1083 and 1079 cm^{-1} are attributed to Si–O–Si asymmetric stretching vibration confirmatory to the survival of a SiO_2 layer around Fe_3O_4 nanoparticles. The bands centered at 1615–1630 and 1509 cm^{-1} were attributed to the bending vibrations of O–H and N–H bonds, respectively. Also, the asymmetric stretching vibrations of O–H and N–H groups appeared at 3467 and 3191 cm^{-1}, respectively. The appearance of the bands at 2958 and 2851 cm^{-1} assigned for the asymmetric and symmetric C–H stretching vibrations, respectively, combined with the appearance of the S=O stretching vibration band at 1207 and 1127 cm^{-1}, and also the increase in the intensities of the band at 3422 cm^{-1} as shown in Figure 1(c) confirms that the sulfonated amine-functionalized propyl moieties are successfully anchored on the surface of the silica-coated Fe_3O_4 NPs.

As shown in Figure 2, the SEM image indicates that the prepared Fe_3O_4@SiO_2@N(SO_3H)-NH(SO_3H) nanoparticles possess an average diameter of about 41 nm and the catalyst is made up of core-shell structure with spherical morphology. Also, the SEM image shows that the size and morphology of the Fe_3O_4@SiO_2@N(SO_3H)-NH(SO_3H) NPs were not noticeably changed in comparison with the ungrafted Fe_3O_4 nanoparticles.[30]

The components of the Fe_3O_4@SiO_2-Cl nanoparticles were characterized by using XRF analysis. The XRF spectrum of the Fe_3O_4@SiO_2-Cl shown in Figure 3 exhibits the elemental composition (Si, Cl and Fe).

Moreover, as shown in Figure 4, the EDX was obtained from the synthesized catalyst Fe_3O_4@SiO_2@N(SO_3H)-NH(SO_3H) in which the expected elemental composition (C, N, O, Si, S, Fe) is shown clearly.

Figure 5 presents the crystalline structure of Fe_3O_4@SiO_2@N(SO_3H)-NH(SO_3H) nanoparticles identified with the XRD technique. The diffraction peaks are appeared with $2\theta = 30.0°$, 35.7°, 43.7°, 53.6°, 57.4° and 62.6°. As shown in this figure, the positions and relative intensities of the peaks match well with those of the unfunctionalized Fe_3O_4 nanoparticles.[31] In this XRD pattern of Fe_3O_4@SiO_2@N(SO_3H)-NH(SO_3H), the characteristic peaks of Fe_3O_4 did not show any significant change except that the

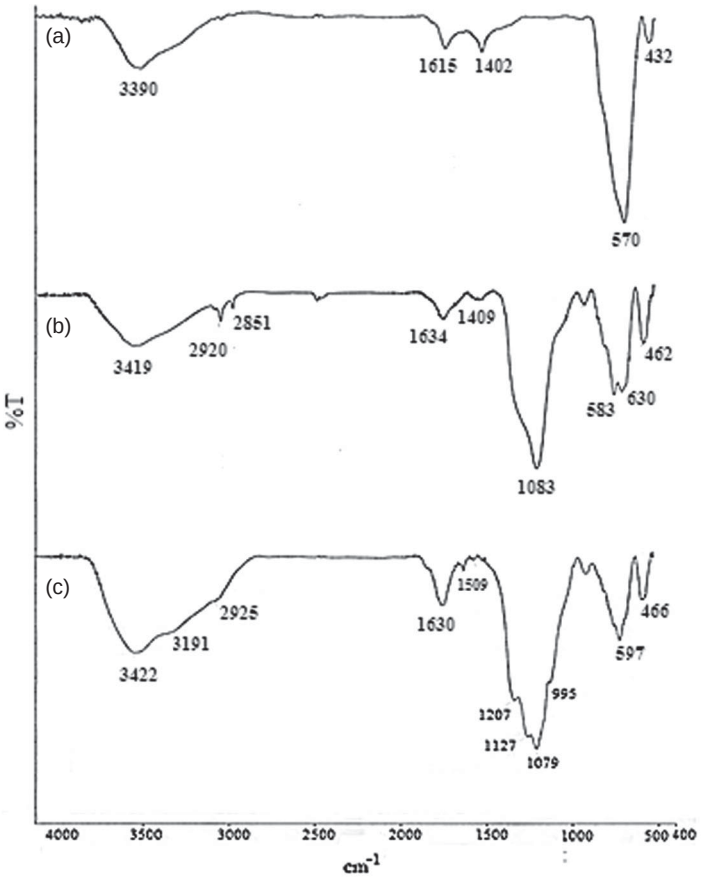

Figure 1. FT-IR spectra of synthesized Fe_3O_4 NPs (a), Fe_3O_4@SiO_2-Cl (b) and Fe_3O_4@SiO_2@N(SO_3H)-NH(SO_3H) NPs (c).

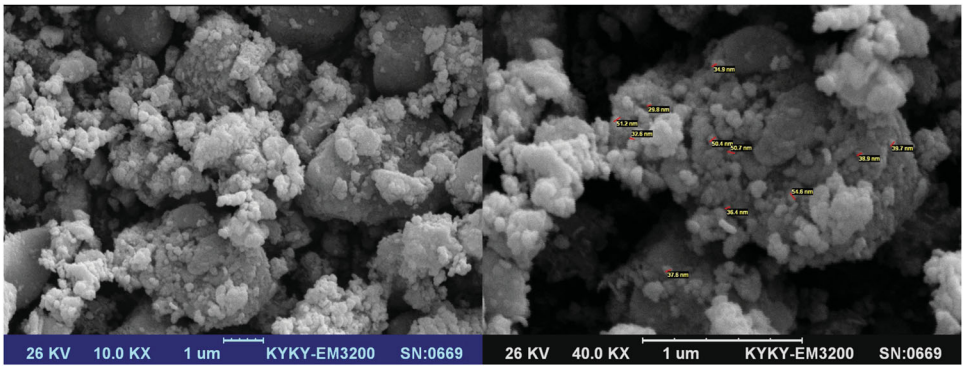

Figure 2. SEM images of Fe_3O_4@SiO_2@N(SO_3H)-NH(SO_3H) NPs.

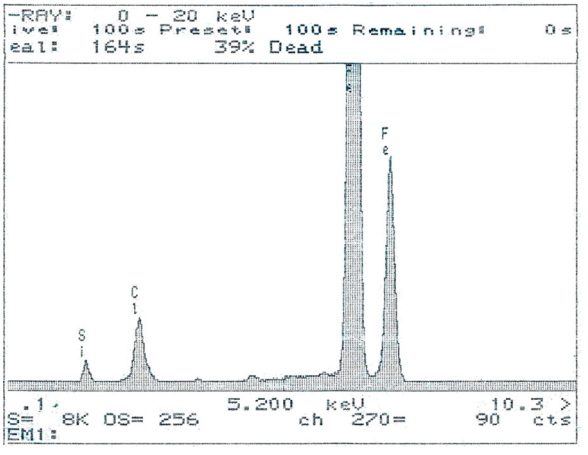

Figure 3. The XRF spectrum of the prepared Fe_3O_4@SiO_2-Cl NPs.

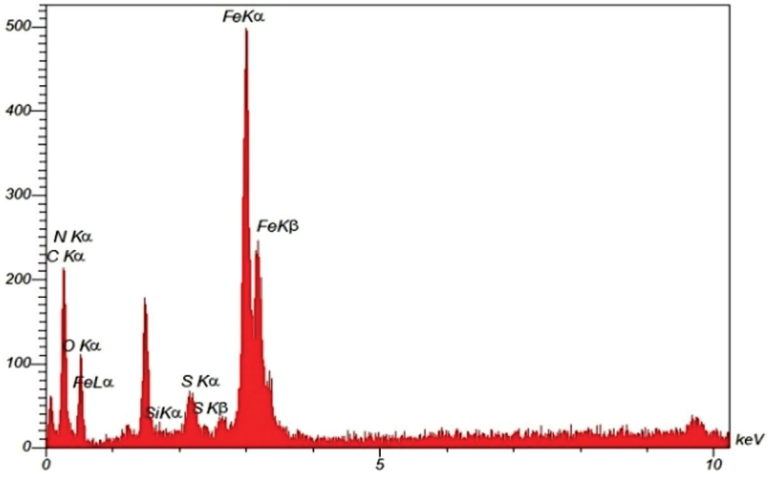

Figure 4. The EDX spectrum of Fe_3O_4@SiO_2@N(SO_3H)-NH(SO_3H) NPs.

intensities and width of the peaks were slightly decreased after being modified with SO_3H groups.

To evaluate the catalytic activity of Fe_3O_4@SiO_2@N(SO_3H)-NH(SO_3H) in the synthesis of 4*H*-chromenes, we initially studied the one-pot three-component reaction between benzaldehyde, malononitrile and 5,5-dimethyl-1,3- cyclohexanedione (dimedone) as simple model reaction. To establish the reaction conditions, the effects of the catalyst loading, solvent and temperature on the rate and yield of this model reaction were investigated. The results summarized in Table 1 clearly indicate that the best results in terms of the reaction rates and yields are obtained when the reaction was carried out using the mixture of equal volumes of EtOH and H_2O as the solvent of choice under reflux conditions with a catalyst loading of 0.01 g (entry 8). In addition, the important role of the catalyst in the reaction was approved by repeating the reaction in the absence of the catalyst with optimal conditions and noting that a trace amount of the expected product was formed and only slight

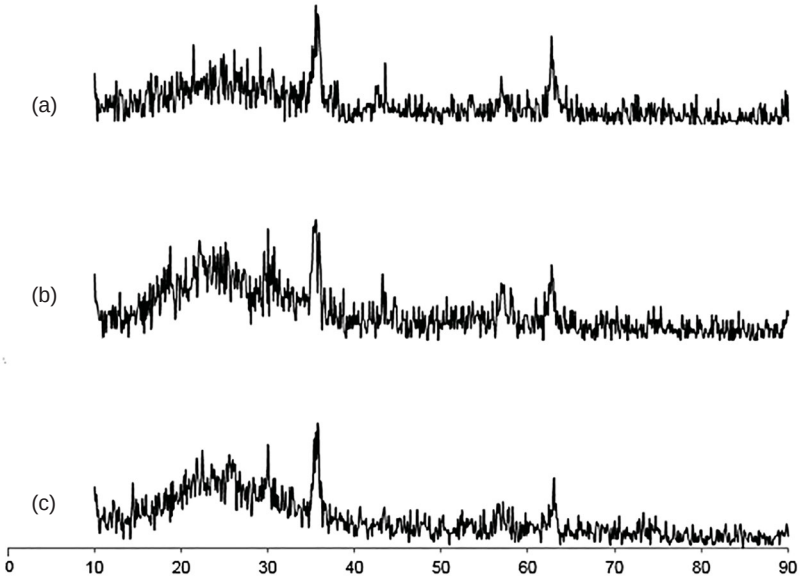

Figure 5. XRD pattern of Fe_3O_4, Fe_3O_4@SiO_2, Fe_3O_4@SiO_2@N(SO_3H)-NH(SO_3H) NPs.

Table 1. Screening the reaction parameters for the model synthesis of 2-amino-7,7-dimethyl-5-oxo-4-phenyl-5,6,7,8-tetrahydro-4*H*-chromene-3-carbonitrile.[a]

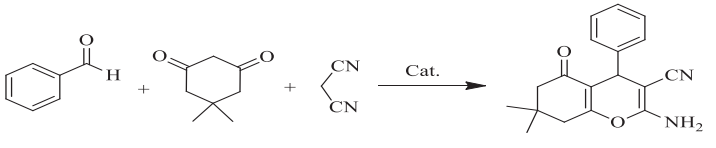

Entry	Catalyst (g)	Solvent[b]	Temperature (°C)	Time (min)	Yield (%)[c]
1	0.01	No solvent	r.t.	120	25
2	0.01	H_2O	r.t.	120	48
3	0.01	EtOH	r.t.	120	54
4	0.01	EtOH/H_2O	r.t.	60	67
5	0.01	EtOH/H_2O	50	60	75
6	0.01	EtOH/H_2O	Reflux	60	96
7	0.01	EtOH/H_2O	Reflux	30	98
8	0.01	EtOH/H_2O	Reflux	10	98
9	0.01	EtOH/H_2O	Reflux	5	95
10	0.02	EtOH/H_2O	Reflux	10	96
11	0.03	EtOH/H_2O	Reflux	10	95
12	No catalyst	EtOH/H_2O	Reflux	10	trace
13	No catalyst	EtOH/H_2O	Reflux	90	15

[a]Conditions: benzaldehyde (1 mmol), 5,5-dimethyl-1,3- cyclohexanedione (1 mmol), malononitrile (1.2 mmol) and solvent (5 mL).
[b]The solvent ratio used for EtOH/H_2O is 2.5 mL:2.5 mL.
[c]Isolated pure yield.

improvement of the yield was observed after a prolonged reaction time of 90 min (entries 12, 13).

Moreover, versatility and the catalytic potential of the catalyst were similarly explored in the synthesis 3,4-dihydropyrimidin-2(1*H*)-ones using the one-pot three-component

Table 2. Screening the reaction parameters for the model synthesis of 5-methoxycarbonyl-6-methyl-4-phenyl-3,4-dihydropyrimidin-2(1*H*)-one.[a]

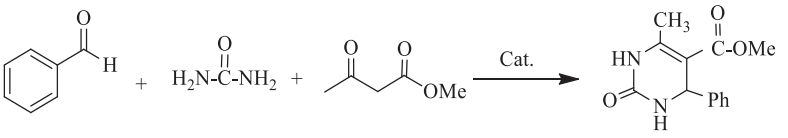

Entry	Catalyst (g)	Solvent	Temperature (°C)	Time (h)	Yield (%)[b]
1	0.01	No solvent	r.t.	8	46
2	0.01	H_2O	r.t.	8	12
3	0.01	EtOH	r.t.	8	30
4	0.02	No solvent	r.t.	8	45
5	0.02	H_2O	r.t.	8	15
6	0.02	EtOH	r.t.	8	28
7	0.03	No solvent	r.t.	8	45
8	0.01	No solvent	50	4	70
9	0.01	No solvent	80	4	80
10	0.01	No solvent	100	4	94
11	0.01	No solvent	100	1	96
12	0.01	No solvent	100	0.5	96
13	No catalyst	No solvent	100	5	trace

[a]Conditions: benzaldehyde (1 mmol), methyl acetoacetate (1 mmol), urea (1.5 mmol), solvent (5 mL).
[b]Isolated pure yield.

condensation reaction of benzaldehyde, methyl acetoacetate and urea as the model reaction. To establish the reaction conditions, we studied the effects of the same green solvents H_2O and EtOH, catalyst loading and reaction temperature on the reaction. According to the results summarized in Table 2, the optimal results for the reaction are obtained in the absence of solvent using a catalyst loading of 0.01 g at 100°C (entry 12). The value of the catalyst in the reaction was substantiated by conducting the reaction in the absence of the catalyst that resulted in no detectable amount of the expected product with almost full recovery of the starting materials even after a prolonged reaction time (entry 13).

To develop the scope of the reactions, we conducted these reactions with a series of aldehydes under the optimized conditions (a catalyst loading of 0.01 g, solvent-free, reaction temperature of 100°C for the synthesis of 3,4-dihydropyrimidinones, and the catalyst loading of 0.01 g, and H_2O/EtOH mixture as the solvent under reflux condition for the synthesis of 4*H*-chromenes); the results are summarized in Tables 3 and 4, respectively. As shown in these tables, the aldehydes carrying electron-donating and electron-withdrawing groups all undergo these reactions to afford the respective products in excellent yields irrespective of the nature of the substituent groups. All the products were characterized by their physical properties and spectral (FT-IR, ^{1}H NMR and ^{13}C NMR) analysis which were in accord with those reported in the literature. The characteristic data for some selected products are presented in the Experimental section.

2.1. Proposed catalytic reaction mechanisms

A possible mechanism to explain the formation of 4*H*-chromenes is depicted in Scheme 3. It is likely that the initial step involves the Fe_3O_4@SiO_2@N(SO_3H)-NH(SO_3H)-catalyzed condensation of the aldehyde with malononitrile followed by dehydration to produce

Table 3. Synthesis of 3,4-dihydropyrimidin-2(1*H*)-ones **2a–2l** catalyzed by nonmagnetic catalyst Fe_3O_4@SiO_2@ N $(SO_3H)NH(SO_3H)$ under solvent-free conditions.[a]

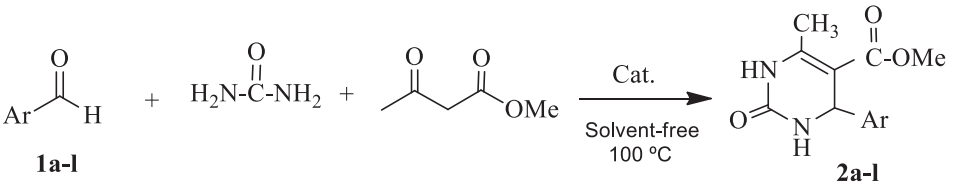

Entry	Ar	Product	Time (min)	Yield (%)[b]	M.p. (°C) Found	M.p. (°C) Reported
1	C_6H_5	**2a**	30	85	213–215	208–211[33]
2	2-ClC_6H_4	**2b**	35	79	248–251	252–253[34]
3	4-ClC_6H_4	**2c**	30	87	206–208	204–206[34]
4	4-FC_6H_4	**2d**	35	83	197–200	192–194[35]
5	4-MeC_6H_4	**2e**	20	95	207–211	206–209[33]
6	4-HOC_6H_4	**2f**	40	87	238–240	235–237[33]
7	2-$MeOC_6H_4$	**2g**	30	81	285–287	284–286[33]
8	3-ClC_6H_4	**2h**	30	85	210–213	208–211[33]
9[new]	2,5-$(MeO)_2C_6H_3$	**2i**	35	91	236–240	–
10[new]	$C_6H_5(CH_2)_2$	**2j**	35	89	138–140	–
11[new]	3-C_5H_4N	**2k**	40	87	200–203	–
12	2-C_4H_4S	**2l**	40	89	189–191	–

[a]Conditions: aldehyde (1 mmol), methyl acetoacetate(1 mmol), urea(1.5 mmol), catalyst (0.01 g).
[b]Isolated pure yield.

Table 4. Synthesis of 4*H*-chromenes **3a–3k** catalyzed by nonmagnetic catalyst Fe_3O_4@SiO_2@N $(SO_3H)NH(SO_3H)$ in EtOH/H_2O at the reflux temperature.[a]

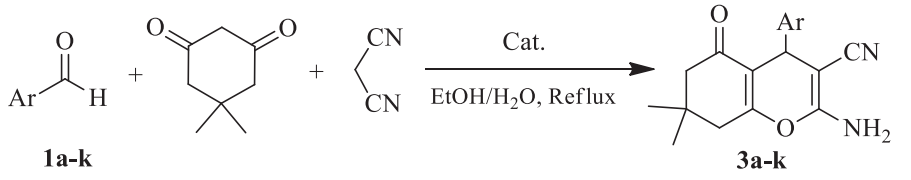

Entry	Ar	Product	Time (min)	Yield (%)[b]	M.p. (°C) Found	M.p. (°C) Reported
1	C_6H_5	**3a**	10	96	231–233	227–229[36]
2	4-BrC_6H_4	**3b**	35	90	196–198	199–200[37]
3	2-ClC_6H_4	**3c**	20	91	211–214	217–218[38]
4	3-ClC_6H_4	**3d**	25	89	211–213	224–225[36]
5	4-ClC_6H_4	**3e**	10	98	216–218	212–214[36]
6	4-FC_6H_4	**3f**	30	88	194–196	192–194[37]
7	4-MeC_6H_4	**3g**	15	95	211–213	212–215[36]
8	4-HOC_6H_4	**3h**	35	86	209–211	212–215[37]
9	4- $NO_2C_6H_4$	**3i**	20	91	182–185	178–180[38]
10	3-$NO_2C_6H_4$	**3j**	20	95	216–218	210–212[36]
11	2-C_4H_4S	**3k**	30	94	200–202	–

[a]Conditions: aldehyde (1 mmol), 5,5-dimethyl-1,3- cyclohexanedione (1 mmol), malononitrile (1.2 mmol), EtOH/H_2O (2.5 mL/2.5 mL), catalyst (0.01 g).
[b]Isolated pure yield.

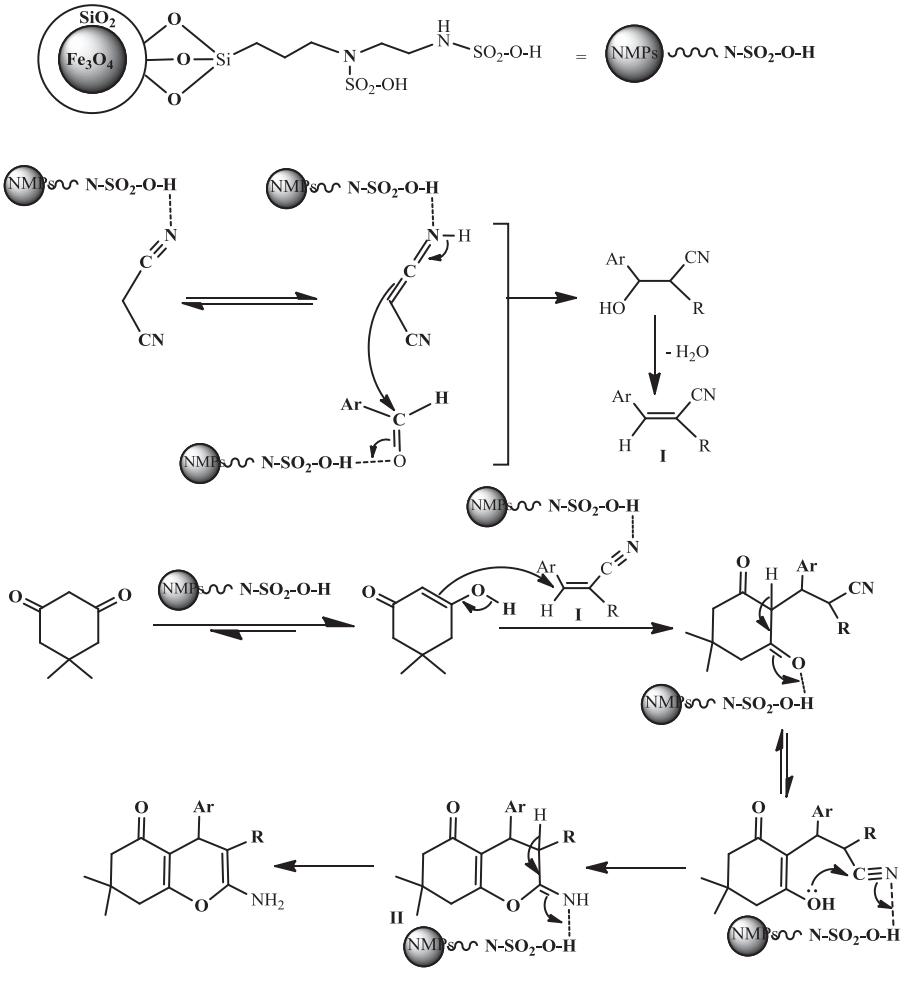

Scheme 3. A possible reaction path way for the synthesis of tetrahydrobenzo[b]pyran derivatives catalyzed by Fe_3O_4@SiO_2@N(SO_3H)-NH(SO_3H) MNPs.

the arylidenemalononitrile intermediate **I**. Subsequently, the catalyst-induced nucleophilic addition of the enolizable dimedone to the intermediate **I** followed by consecutive intramolecular cyclization occurs to provide the intermediate **II** which rearranges to afford the expected product 4*H*-chromene.

Similarly, a plausible reaction mechanism suggested for the synthesis of dihydropyrimidinones in the presence of the same catalyst is illustrated in Scheme 4. Initially, the aldehyde is activated by the catalyst and undergoes the electrophilic addition with urea followed by dehydration to provide the intermediate **I**. On the other hand, the methyl acetoacetate is enolized in the presence of the catalyst to yield the intermediate **II** which reacts with the intermediate **I** in an Aldol-type reaction to produce the intermediate **III**. Sequentially, the intermediate **III** undergoes annulation and dehydration to produce the expected products.

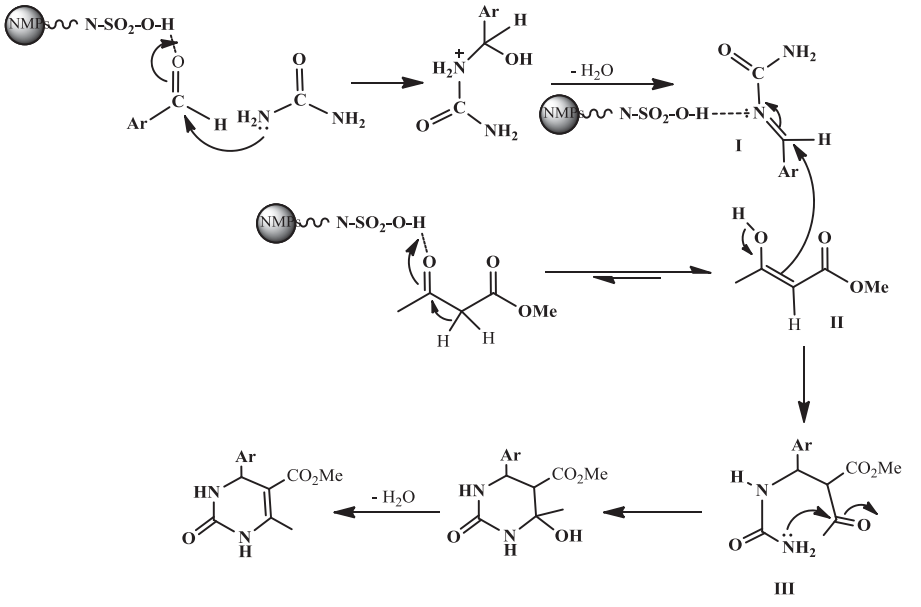

Scheme 4. A possible reaction path way for the catalytic synthesis of dihydropyrimidinones catalyzed by Fe_3O_4@SiO_2@N(SO_3H)-NH(SO_3H).

2.2. Catalyst recyclability

The catalytic recyclability of the catalyst Fe_3O_4@SiO_2@N(SO_3H)-NH(SO_3H) was examined for the model reaction of benzaldehyde, dimedone and malononitrile. The recycling process involved the isolation of the catalyst from the reaction mixture simply by using a magnet bar. The recovered catalyst was purified by washing with ethyl acetate followed by drying in an oven. The results summarized in Figure 6 indicate that the catalyst can be used

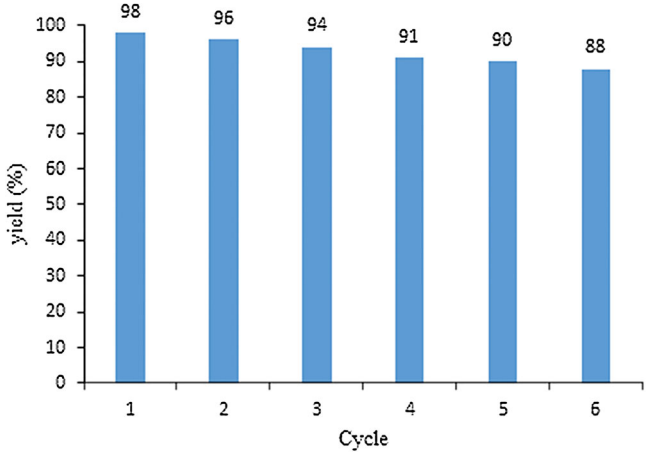

Figure 6. Catalytic reusability of Fe_3O_4@SiO_2@N(SO_3H)-NH(SO_3H) NPs for the synthesis of 4*H*-chromenes.

for five consecutive times without the noticeable loss of catalytic activity. The integrity of the recovered catalyst was examined and proved to be as active as the originally used catalyst. Moreover, the XRD analysis of the recovered catalyst indicated that its structural integrity remains intact after separation from the reaction mixture.

3. Conclusion

In this research, Fe_3O_4@SiO_2@N(SO_3H)-NH(SO_3H) magnetic nanocomposite was successfully prepared and characterized by FT-IR, SEM, XRF, EDX and XRD analyses. The catalytic activity of this solid acid nanocomposite was probed through the one-pot synthesis of 3,4-dihydropyrimidin-2(1*H*)-ones and tetrahydrobenzo[b]pyran derivatives by three-component reactions of aldehydes with acetoacetate, urea or malononitrile and dimedone, respectively. The attractive features of this method are simple procedure, cleaner reaction, easy recyclability and reusability of the catalyst, easy workup and performing multicomponent reactions under solvent-free conditions for the synthesis of dihydropyrimidin-2(1*H*)-ones or the use of green solvents for the synthesis of 4*H*-chromenes.

4. Experimental

4.1. General remarks

FT-IR spectra were recorded on a Shimadzu 435-U-04 FT spectrometer (KB pellets). NMR spectra were recorded on 300 MHz BRUKER and 90 MHz JEOL FX 90Q spectrometers in $CDCl_3$ (or DMSO-d_6). Melting points were determined in open capillary tubes using a BUCHI 510 apparatus. SEM was performed on a KYKY-EM3200 instrument operated at 26 kV accelerating voltage. The XRD was recorded on a ITAL APD 2000 powder diffractometer equipped with Cu K_α radiation ($\lambda = 1.54056$ Å) operated at 40 kV and 30 mA, at a scanning speed of 2 s from 10° to 90° (2θ). Qualitative analysis of the Fe_3O_4@SiO_2-Cl sample was performed by using energy-dispersive X-ray fluorescence spectroscopy (Brand: Link analytical XR300). EDX analysis of the prepared catalyst was performed on a SEM-TESCAN MIRA3-FEG instrument. The elemental analyses (C, H, N, S) were obtained from a Vario El Series II elemental analyzer flowchart. Ultrasonication was performed in a 2200 ETH-SONICA ultrasound cleaner with a frequency of 45 kHz.

4.2. Synthesis of the catalyst

4.2.1. Synthesis of magnetic Fe_3O_4 nanoparticles

First, Fe_3O_4 nanoparticles were prepared by co-precipitation of Fe^{+2} and Fe^{+3} ions with a molar ratio of 1:2 following the reported method.[28] $FeCl_2{\cdot}4H_2O$ (1.790 g, 9.0 mmol) and $FeCl_3{\cdot}6H_2O$ (4.865 g, 18 mmol) were dissolved in 100 mL deionized water and ultrasonicated twice for 15 min each time under N_2 atmosphere. Then, an aqueous 25% NH_4OH solution (10 mL) was immediately added to the mixture under nitrogen gas and vigorously stirred for a further 30 min at room temperature. The resulting black precipitate was isolated and washed twice with distilled water and twice with 0.02 M NaCl aqueous solution. Magnetic Fe_3O_4 nanoparticles were separated in an external magnetic field and

dried under vacuum. The FT–IR spectra of the prepared Fe_3O_4 nanoparticles are shown in Figure 1(a).

4.2.2. Synthesis of silica-coated magnetite Fe_3O_4 nanoparticles (Fe_3O_4@SiO_2)

According to the previously reported method,[29] 30 mL of 0.2 M citric acid solution was added to 1 g of the prepared magnetic Fe_3O_4 nanoparticles and the mixture was ultrasonicated for 30 min. Then, the pH value of the mixture was adjusted to 5.2 by adding 0.4 mL of aqueous ammonia solution. The reaction mixture was stirred under reflux condition for 90 min. The resulting reaction mixture was cooled to room temperature and 2 mL of ammonia solution was added until the pH value was reached to 11. Then, a solution of 1.2 mL tetraethyl orthosilicate in 12 mL ethanol was added dropwise and the resulted mixture was sonicated for 30 min at room temperature followed by refluxing for 24 h. The resulting solid Fe_3O_4@SiO_2 nanoparticles were successively washed with ethanol and deionized water. Finally, the dark brown precipitate was separated in a magnetic field and dried in vacuum.

4.2.3. Synthesis of chloropropyl-modified silica-coated magnetite nanoparticles (Fe_3O_4@SiO_2-Cl)

Chloropropyl modification of the magnetite Fe_3O_4 nanoparticles (Fe_3O_4@SiO_2) was carried out according to the reported method.[32] The Fe_3O_4@SiO_2 (1 g) was dispersed in 50 mL of dry xylene and ultrasonicated for 60 min. Then, 3-chloropropyltrimethoxysilan (1.8 mL, 10 mmol) was added dropwise to the dispersion and ultrasonicated for 30 min. The resulted mixture was subsequently refluxed at 140°C under vigorous stirring for 24 h. The resulted bright brown nanoparticles were magnetically separated, consecutively washed twice with dry xylene and twice with ethanol, and then dried at 60°C. The FT–IR spectrum obtained from the prepared Fe_3O_4@SiO_2-Cl nanoparticles is given in Figure 1(b). Also, the XRF of the Fe_3O_4@SiO_2-Cl shown in Figure 3 exhibits the elemental composition (Si, Cl, Fe).

4.2.4. Synthesis of diamine-functionalized silica-coated magnetite nanoparticles (Fe_3O_4@SiO_2@NH-NH_2)

A dispersion of 1 g of Fe_3O_4@SiO_2-Cl in 50 mL of CH_3CN was ultrasonicated for 30 min. Subsequently, 1 mL ethylene diamine (15 mmol) and 0.1 mL of triethyl amine were added dropwise to the reaction mixture and refluxed for 24 h. The resulted solid product was separated from the solution using a magnet bar, washed with water/ethanol, and finally dried at 60°C.

4.2.5. Conversion of the Fe_3O_4@SiO_2@$NHNH_2$ MNPs into the disulfonated derivative Fe_3O_4@SiO_2@N(SO_3H)NH(SO_3H) MNPs

A dispersion of 1 g of the prepared magnetite Fe_3O_4@SiO_2@NH-NH_2 nanoparticles in 50 mL chloroform was ultrasonicated for 15 min. Then, chlorosulfonic acid (0.8 mL, 12 mmol) was added dropwise and the resulting reaction mixture was stirred for 4 h. The resulted brick-red powder was successively separated by using a magnet bar, washed with ethanol (3 × 30 mL) to remove the remaining acid, and dried overnight at room temperature. The successful synthesis of this sample was confirmed based on the FT–IR, EDX and elemental analyses.

4.3. General procedure for the synthesis of 3,4-dihydropyrimidin-2(1H)-ones 2a-l using the nanocatalyst Fe_3O_4@SiO_2@N(SO_3H) NH(SO_3H)

To a mixture of methyl acetoacetate (1 mmol), aromatic aldehyde **1** (1 mmol) and urea (1.5 mmol) in a 100 mL round-bottomed flask, the synthesized catalyst (0.01 g) was added and the mixture was mechanically stirred at 100°C for an appropriate time (Table 3). After completion of the reaction as monitored by TLC, 10 mL of ethanol was added to the reaction mixture and stirring was continued at room temperature for 10 min. The catalyst was easily isolated by using a magnet bar and the product was obtained after removal of the solvent under reduced pressure. Then, the product was treated with water followed by crystallization from EtOH. The products were characterized by their physical and spectral (IR, ^{1}H and ^{13}CNMR) analysis and compared with the reported data. The spectral data of the new products are presented below.

4.3.1. 5-Methoxycarbonyl-6-methyl-4-(2,5-dimethoxyphenyl)-3,4-dihydropyrimidin-2(1H)-one (2i)

Chartreuse yellow solid, m.p. 236–240°C; IR (KBr, cm^{-1}): 3243 and 3107 (N–H str.), 2946 (C-H str.) 1710, 1686 (C=O str.), 1643 (C=C str.). ^{1}H NMR (90 MHz, DMSO-d_6) δ: 2.28 (s, 3H, CH_3), 3.48, 3.65 (s, 3H, –$COOCH_3$), 3.74 (s, 6H, –OCH_3), 5.41 (s, 1H, CH), 7.24, 6.85 and 6.55 (m, 4H, Ar–H), 7.70 (s, 1H, NH), 9.14 (s, 1H, NH) ppm. ^{13}CNMR (300 MHz, DMSO-d_6) δ: 18.2, 49.4, 51.2, 55.7, 56.4, 97.7, 112.3, 112.7, 114.2, 132.9, 149.7, 151.1, 152.7, 153.4, 166.2 ppm. Anal. Calcd. for $C_{15}H_{18}N_2O_5$: C, 58.82; H, 5.92; N, 9.15; Found: C, 58.86; H, 5.94; N, 9.18.

4.3.2. 5-Methoxycarbonyl-6-methyl-4-(2-phenylethyl)-3,4-dihydropyrimidin-2(1H)-one (2j)

Cream solid, m.p. 138–140°C; IR (KBr, cm^{-1}): 3252, 3114 (N–H str.), 2949 (C–H str.), 1724, 1686 (C=O str.); 1658 (C=C str.). ^{1}H NMR (90 MHz, DMSO-d_6) δ: 2.16 (s, 3H, CH_3), 1.27 and 2.97 (m, 4H, CH_2CH_2), 3.55 (s, 3H, –OCH_3), 5.17 (s, 1H, CH), 7.20, 7.45 (m, 5H, Ar–H), 7.73 (s, 1H, NH), 9.04 (s, 1H, NH) ppm. ^{13}CNMR (300 MHz, DMSO-d_6) δ: 18.2, 30.4, 50.4, 51.1, 99.3, 126.1, 128.7, 142.0, 149.2, 153.2, 166.3 ppm. Anal. Calcd. for $C_{15}H_{18}N_2O_3$: C, 65.68; H, 6.61; N, 10.21; Found: C, 65.72; H, 6.65; N, 10.26.

4.3.3. 5-Methoxycarbonyl-6-methyl-4-(pyridin-3-yl)-3,4-dihydropyrimidin-2(1H)-one (2k)

Slime green solid, m.p. 200–203°C; IR (KBr, cm^{-1}): 3212 and 3092 (N–H str.), 2949 (C–H str.), 1707, 1677 (C=O str.), 1648 (C=C str.). ^{1}H NMR (90 MHz, DMSO-d_6) δ: 2.28 (s, 3H, CH_3), 3.53 (s, 3H, –OCH_3), 5.20 (s, 1H, CH), 7.38, 7.58, 7.80 (m, 4H, Ar–H), 8.44 (s, 1H, NH), 9.33 (s, 1H, NH) ppm. ^{13}CNMR (22.5 MHz, DMSO-d_6) δ: 17.8, 50.8, 51.9, 57.6, 98.1, 123.8, 133.8, 139.8, 147.8, 151.9, 157.7, 165.5 ppm. Anal. Calcd. for $C_{12}H_{13}N_3O_3$: C, 58.29; H, 5.30; N, 16.99; Found: C, 58.34; H, 5.37; N, 17.05.

4.3.4. 5-Methoxycarbonyl-6-methyl-4-(thiophen-2-yl)-3,4-dihydropyrimidin-2(1H)-one (2l)

Cream solid, m.p. 189–191°C; IR (KBr, cm^{-1}): 3440–3115 (N–H str.), 2948 (C–H str.), 1690, 1642 (C=O str.); 1607 (C=C str.). ^{1}H NMR (400 MHz, DMSO-d_6) δ: 2.2 (s, 3H,

CH_3), 3.6 (s, 3H, $-OCH_3$), 5.4 (s, 1H, CH), 6.91, 6.95 (m, 2H, Ar–H), 7.3 (s, H, H-CS), 7.9 (s, 1H, NH), 9.4 (s, 1H, NH) ppm. ^{13}CNMR (400 MHz, DMSO-d_6) δ: 18.2, 49.7, 51.4, 100.0, 124.0, 125.1, 127.2, 149.1, 152.8, 160.3, 165.9 ppm. Anal. Calcd. for $C_{11}H_{12}N_2O_3S$: C, 52.37; H, 4.79; N, 11.10; S, 12.71; Found: C, 52.45; H, 4.85; N, 11.16; S, 12.42.

4.4. General procedure for the synthesis of 4H-chromenes 3a–3k using the nanocatalyst Fe_3O_4@SiO_2@N(SO_3H)NH(SO_3H)

To a mixture of aromatic aldehyde **1** (1 mmol), malononitrile (1.2 mmol) and dimedone (1 mmol) in the mixed solvent EtOH (2.5 mL)/H_2O (2.5 mL) was added the nanocatalyst (0.01 g) and the resulting mixture was stirred at the reflux temperature for an appropriate time (Table 4). After completion of the reaction as monitored by TLC, 10 mL hot ethanol was added to the reaction mixture and stirring was continued for further 10 min. Then, the catalyst was separated from the reaction mixture simply by using an external magnet bar. The remaining solution was diluted with 50 mL of water and filtered to collect the solid products which were dried under vacuum. Crystallization in 96% ethanol provided the pure products. The structures of the products were established on the basis of their physical and spectral (IR, ^{1}H NMR and ^{13}CNMR) data which were in accord with those reported in the literature. A number of selected data are presented below.

4.4.1. 2-Amino-4-(3-chlorophenyl)-7,7-dimethyl-5-oxo-5,6,7,8-tetrahydro-4H-chromene-3-carbonitrile (3d)

White solid, m.p. 211–213°C, IR (KBr, cm^{-1}): 3394, 3329, 3198, 2960, 2199, 1682, 1654, 1604, 1370, 1214. ^{1}H NMR (90 MHz, DMSO-d_6) δ: 1.07 (s, 6H, CH_3), 2.21 (s, 2H, CH_2), 2.44 (s, 2H, CH_2), 4.65 (s, 2H, NH_2), 4.84 (s, 1H, CH), 7.192 (s, 4H, H–Ar) ppm. ^{13}C NMR (22.5 MHz DMSO-d_6) δ: 196.3, 163.4, 159.0, 147.6, 133.3, 130.8, 127.5, 127.1, 126.4, 120.0, 112.5, 58.0, 50.3, 35.7, 32.3, 28.7, 27.2 ppm.

4.4.2. 2-Amino-4-(4-hydroxyphenyl)-7,7-dimethyl-5-oxo-5,6,7,8-tetrahydro-4H-chromene-3-carbonitrile (3h)

White solid, m.p. 209–211°C, IR (KBr, cm^{-1}): 3362, 3331, 3193, 2964, 2894, 2193, 1682, 1651, 1605, 1371, 1215. ^{1}H NMR (90 MHz, DMSO) δ: 0.90 (s, 3H, CH_3), 0.97 (s, 3H, CH_3), 2.13 (s, 2H, CH_2), 2.44 (s, 2H, CH_2), 4.00 (s, 1H, CH), 6.63 (s, 2H, NH_2), 6.84 (s, 4H, H–Ar), 9.19 (s, 1H, OH) ppm. ^{13}C NMR (22.5 MHz DMSO-d_6) δ: 196.4, 163.4, 159.2, 156.0, 135.4, 128.5, 122.2, 115.5, 114.6, 59.9, 50.6, 41.4, 34.3, 33.2, 29.2, 27.4 ppm.

4.4.3. 2-Amino-7,7-dimethyl-4-(4-nitrophenyl)-5-oxo-5,6,7,8-tetrahydro-4H-chromene-3-carbonitrile (3i)

Cream solid, m.p. 182–185°C, IR (KBr, cm^{-1}): 3451, 3374, 3333, 3257, 3216, 2960, 2876, 2196, 1688, 1671, 1594, 1520, 1362, 1218. ^{1}H NMR (90 MHz, DMSO-d_6) δ: 0.96 (s, 3H, CH_3), 1.04 (s, 3H, CH_3), 2.17 (s, 2H, CH_2), 2.53 (s, 2H, CH_2), 4.37 (s, 1H, CH), 7.18 (m, 4H, H–Ar), 8.12 (s, 2H, NH_2) ppm. ^{13}C NMR (22.5 MHz, DMSO-d_6) δ: 195.8, 162.9, 158.7, 152.3, 146.3, 128.5, 124.1, 119.3, 112.1, 57.1, 49.9, 35.7, 34.5, 28.3, 27.1 ppm.

4.4.4. 2-Amino-7,7-dimethyl-5-oxo-4-(thiophen-2-yl)-5,6,7,8-tetrahydro-4H-chromene-3-carbonitrile (3k)

White solid, m.p. 200–202°C, IR (KBr, cm^{-1}): 3382, 3321, 3208, 2963, 2878, 2198, 1678, 1660, 1602,1466, 1374,1214. ^{1}H NMR (400 MHz, DMSO-d_6) δ: 0.98 (s, 3H, CH_3), 1.05 (s, 3H, CH_3), 2.1–2.2 (s, 2H, CH_2), 2.4–2.5 (s, 2H, CH_2), 4.5 (s, 1H, CH), 6.6–6.9 (m, 2H, H-Ar), 7.1–7.3 (s, H, H-CS, s, 2H, NH_2) ppm. ^{13}C NMR (400 MHz DMSO-d_6) δ: 195.51, 162.47, 158.87, 149.25, 126.78, 124.39, 123.97, 119.58, 112.88, 57.99, 49.83, 31.71, 30.37, 28.61, 26.42 ppm. Anal. Calcd. for $C_{16}H_{16}N_2O_2S$: C, 63.98; H, 5.37; N, 9.33; S, 10.67; Found: C, 64.08.72; H, 5.42; N, 9.38; S, 10.62.

Funding information

The authors wish to thank the Research Council of the Bu-Ali Sina University (Iran) for the financial support to carry out this research.

ORCID details

Davood Azarifar http://orcid.org/0000-0002-7331-2748

References

[1] Faraji MV, Yamini YV, Rezaee MV. Magnetic nanoparticles: synthesis, stabilization, functionalization, characterization, and applications. J Iran Chem Soc. 2010;7:1–37.
[2] Rossi LM, Costa NJS, Silva FP, Goncalves RV. Magnetic nanocatalysts: supported metal nanoparticles for catalytic applications. Nanotech Rev. 2013;2:597–614.
[3] Wang SJ, Wang ZY, Zha ZG. Metal nanoparticles or metal oxide nanoparticles, an efficient and promising family of novel heterogeneous catalysts in organic synthesis. Dalton Trans. 2009;43:9363–9373.
[4] Baig RBN, Varma RS. Magnetically retrievable catalysts for organic synthesis. Chem Commun. 2013;49:752–770.
[5] Wu W, He Q, Jiang C. Magnetic iron oxide nanoparticles: synthesis and surface functionalization strategies. Nanoscale Res Lett. 2008;3:397–415.
[6] Hong RY, Feng B, Liu G, et al. Preparation and characterization of Fe_3O_4/polystyrene composite particles via inverse emulsion polymerization. J Alloys Compd. 2009;476:612–618.
[7] Hamadia H, Kootia M, Afsharia M, Ghiasifarb Z, Adibpourc N. Magnetic nanoparticle supported polyoxometalate: An efficient and reusable catalyst for solvent-free synthesis of α-aminophosphonates. J Mol Catal A: Chem. 2013;373:25–29.
[8] Sadat H, Nazifi Z. A highly efficient nano-Fe_3O_4 encapsulated-silica particles bearing sulfonic acid groups as a solid acid catalyst for synthesis of 1,8-dioxo-octahydroxanthene derivatives. J Nanopart Res. 2013;15:2026–2036.
[9] Jetti SR, Bhatewara A, Kadre T, Jain S. Silica-bonded *N*-propyl sulfamic acid as an efficient recyclable catalyst for the synthesis of 3,4-dihydropyrimidin-2-(1*H*)-ones/thiones under heterogeneous conditions. Chin Chem Lett. 2014;25:469–473.
[10] Shahbazi F, Amani K. Synthesis, characterization and heterogeneous catalytic activity of diamine-modified silica-coated magnetite-polyoxometalate nanoparticles as a novel magnetically-recoverable nanocatalyst. Catal Commun. 2014;55:57–64.
[11] Rahi T, Baghernejad M, Niknam K. Silica-bonded *N*-propyl diethylenetriamine sulfamic acid as a recyclable solid acid catalyst for the synthesis of α-aminonitriles. Chin J Catal. 2012;33:1095–1100.
[12] Kappe CO. Biologically active dihydropyrimidones of the Biginili type, a literature survey. Eur J Med Chem. 2000;35:1043–1052.

[13] Grover GJ, Dzwonczyk S, McMullen DM, et al. Pharmacologic profile of the dihydropyrimidine calcium channel blockers SQ 32,547 and SQ 32,946. J Cardiovasc Pharmacol. 1995;26:289–294.
[14] Gartner M, Sunder-Plassmann N, Seiler J, et al. Development and biological evaluation of potent and specific inhibitors of mitotic Kinesin Eg_5. Chem Bio Chem. 2005;6:1173–1177.
[15] Biginelli P. Ueber aldehyduramide des acetessigäthers. Ber Dtsch Chem Ges. 1891;24:1317–1319.
[16] Biginelli P. Ueber aldehyduramide des acetessigäthers. II. Ber Dtsch Chem Ges. 1891;24:2962–2967.
[17] Fazaeli R, Tangestaninejad S, Aliyan H, Moghadam M. One-pot synthesis of dihydropyrimidinones using facile and reusable polyoxometalate catalysts for the Biginelli reaction. Appl Catal A. 2006;309:44–51.
[18] Kumar D, Reddy VB, Sharad S, Dube U, Kapur S. A facile one-pot green synthesis and antibacterial activity of 2-amino-4*H*-pyrans and 2-amino-5-oxo-5,6,7,8-tetrahydro-4*H*-chromenes. Eur J Med Chem. 2009;44:3805–3809.
[19] Peng Y, Song G. Amino-functionalized ionic liquid as catalytically active solvent for microwave-assisted synthesis of 4*H*-pyrans. Catal Commun. 2007;8:111–114.
[20] Jin TS, Liu LB, Zhao Y, Li Clean TS. One-pot synthesis of 4*H*-Pyran derivatives catalyzed by hexadecyltrimethyl ammonium bromide in aqueous media. Synth Commun. 2005;35:1859–1863.
[21] Seshu BN, Pasha N, Venkateswara RKT, Sai PPS, Lingaiah N. A heterogeneous strong basic Mg/La mixed oxide catalyst for efficient synthesis of polyfunctionalized pyrans. Tetrahedron Lett. 2008;49:2730–2733.
[22] Banerjee S, Horn A, Khatri H, Sereda G. A green one-pot multicomponent synthesis of 4*H*-pyrans and polysubstituted aniline derivatives of biological, pharmacological, and optical applications using silica nanoparticles as reusable catalyst. Tetrahedron Lett. 2011;52:1878–1881.
[23] Kaupp G, Naimi-Jamal MR, Schmeyers J. Solvent-free Knoevenagel condensations and Michael additions in the solid state and in the melt with quantitative yield. Tetrahedron. 2003;59:3753–3760.
[24] Fotouhi L, Heravi MM, Fatehi A, Bakhtiari K. Electrogenerated base-promoted synthesis of tetrahydrobenzo[b]pyran derivatives. Tetrahedron Lett. 2007;48:5379–5381.
[25] Azarifar A, Nejat-Yami R, AlKobaisi M, Azarifar D. Magnetic $La_{0.7}Sr_{0.3}MnO_3$ nanoparticles: recyclable and efficient catalyst for ultrasound-accelarated synthesis of 4*H*-chromenes, and 4*H*-pyrano[2,3-c]pyrazoles. J Iran Chem Soc. 2013;10:439–446.
[26] Azarifar D, Khatami SM, Nejat-Yami R. Nano-titania-supported Preyssler-type heteropolyacid: An efficient and reusable catalyst in ultrasound-promoted synthesis of 4*H*-chromenes and 4*H*-pyrano [2,3-c]pyrazoles. J Chem Sci. 2014;126:95–101.
[27] Azarifar D, Nejat-Yami R, Sameri F, Akrami Z. Ultrasonic-promoted one-pot synthesis of 4*H*-chromenes, pyrano[2,3-d]pyrimidines, and 4*H*-pyrano[2,3-c]pyrazoles. Lett Org Chem. 2012;9:435–439.
[28] Jetti SR, Bhatewara A, Kadre T, Jain S. Silica-bonded N-propyl sulfamic acid as an efficient recyclable catalyst for the synthesis of 3,4-dihydropyrimidin-2-(1*H*)-ones/thiones under heterogeneous conditions. Chin Chem Lett. 2014;25:469–473.
[29] Bagherzadeh M, Haghdoost MM, Matlobi-Moghaddam F, et al. Mn(III) complex supported on Fe_3O_4 nanoparticles: magnetically separable nanocatalyst for selective oxidation of thiols to disulfides. J Coord Chem. 2013;66:3025–3036.
[30] Alizadeh A, Khodaei MM, Beygzadeh M, Kordestani D, Feyzi M. Biguanide-functionalized Fe_3O_4/SiO_2 magnetic nanoparticles: an efficient heterogeneous organosuperbase catalyst for various organic transformations in aqueous media. Bull Korean Chem Soc. 2012;33:2546–2552.
[31] Karimi-Jaberi Z, Sadegh Moaddeli M. Synthesis of 3,4-dihydropyrimidin-2(1*H*)-ones and their corresponding 2(1*H*) thiones using trichloroacetic acid as a catalyst under solvent-free

conditions. International Scholarly Research Network, ISRN Organic Chemistry. (2012) ID 474626 4 pages.
[32] Shaabani A, Bazgir A, Teimouri F. Ammonium chloride-catalyzed one-pot synthesis of 3,4-dihydropyrimidin-2-(1*H*)-ones under solvent-free conditions. Tetrahedron Lett. 2003;44:857–859.
[33] Ma Y, Qian Ch, Wang L, Yang M. Lanthanide triflate catalyzed Biginelli reaction. One-pot synthesis of dihydropyrimidinones under solvent-free conditions. J Org Chem. 2000;65:3864–3868.
[34] Mobinikhaledi A, BodaghiFard MA. Tetrabutylammonium bromide in water as a green media for the synthesis of pyrano [2,3-d] pyrimidinone and tetrahydrobenzo[b]pyran derivatives. Acta Chim Slov. 2010;57:931–935.
[35] Abd El-Rahman Naglaa M, Borik Rita M. Eco-friendly solvent-free synthesis of tetrahydrobenzo[b]pyran derivatives under microwave irradiation. World Appl Sci J. 2014;31:1–6.
[36] Jin TS, Wang AQ, Wang X, Zhang JS, Li TS. A clean one-pot synthesis of tetrahydrobenzo[b]pyran derivatives catalyzed by hexadecyltrimethyl ammonium bromide in aqueous media. Synlett. 2004;5:871–873.
[37] Maleki A, Alrezvani Z, Maleki S. Design, preparation and characterization of urea-functionalized Fe_3O_4/SiO_2 magnetic nanocatalyst and application for the one-pot multicomponent synthesis of substituted imidazole derivatives. Catal Commun. 2015;69:29–33.
[38] Zhu J, Wang PCh, Lu M. β-cyclodextrin coated Fe_3O_4 nanoparticles: a simple preparation and application for selective oxidation of alcohols in water. Braz J Chem Soc. 2013;24:171–176.